Antiviral Research 86 (2010) 268–275

Contents lists available at ScienceDirect

Antiviral Research

journal homepage: www.elsevier.com/locate/antiviral

Slow binding–tight binding interaction between benzimidazol-2-one inhibitors and HIV-1 reverse transcriptase containing the lysine 103 to asparagine mutation

Alberta Samuele[a], Emmanuele Crespan[a], Samanta Vitellaro[a], Anna-Maria Monforte[b], Patrizia Logoteta[b], Alba Chimirri[b,*], Giovanni Maga[a,**]

[a] Department of DNA Enzymology and Molecular Virology, Institute of Molecular Genetics-National Research Council, IGM-CNR, via Abbiategrasso 207, 27100 Pavia, Italy
[b] Pharmaceutic and Chemistry Department, University of Messina, Viale Annunziata 98168, Messina, Italy

ARTICLE INFO

Article history:
Received 13 January 2010
Received in revised form 9 March 2010
Accepted 12 March 2010

Keywords:
Antiretroviral therapy
Non-nucleoside HIV-1 reverse transcriptase inhibitors
Drug resistant HIV-1 mutant
Benzimidazolones

ABSTRACT

Novel benzimidazol-2-one non-nucleoside reverse transcriptase inhibitors (NNRTIs) have been recently identified, through rational structure-based molecular modeling and docking approaches, as highly effective inhibitors of the wild type and drug-resistant HIV-1 reverse transcriptase (RT). These compounds also showed potent anti-HIV activities against viral strains, superior to the clinically approved NNRTI efavirenz. However, they were still of limited efficacy towards the K103N mutant. Here we report a detailed enzymatic analysis elucidating the molecular mechanism of interaction between benzimidazol-2-one derivatives and the K103N mutant RT. The loss of potency of these molecules towards the K103N RT was specifically due to a reduction of their association rate to the enzyme. Unexpectedly, these compounds showed a strongly reduced dissociation rate from the K103N mutant, as compared to the wild type enzyme, suggesting that, once occupied by the drug, the mutated binding site could achieve a more stable interaction with these molecules. The characterization of this slow binding–tight binding mutant-specific mechanism of interaction may pave the way to the design of more effective new generation benzimidazol-2-one NNRTIs with promising drug resistant profile and minimal toxicity.

1. Introduction

Human immunodeficiency virus (HIV) is the primary etiological agent of the acquired immunodeficiency syndrome (AIDS). The current highly active anti-retroviral therapy (HAART), based on a combination of three or more reverse transcriptase (RT) and protease inhibitors, proved to be effective in controlling the disease progression and prolonging the survival of affected patients. The nucleoside (NRTIs) and the non-nucleoside (NNRTIs) RT inhibitors are the basic drugs of the HAART regiments (Beale and Robinson, 2000; Sluis-Cremer et al., 2000). The NNRTIs are a heterogeneous class of non-competitive inhibitors, designed to specifically bind to a hydrophobic pocket vicinal to the polymerase catalytic site of the RT (de Béthune, 2010). Most of them showed high specificity against the RT enzyme, low toxicity and favorable pharmacokinetic features, making these drugs the first choice in the initial phases of HAART (Balzarini and De Clercq, 1996; Balzarini et al., 1998, 2004). To date, four NNRTIs have been approved for clinical use: nevirapine, delavirdine, efavirenz and etravirine (Maggiolo, 2009). The rapid emergence of RT mutants, yielding drug-resistant HIV-1 strains, and the occurrence of adverse side effects frequently impair the efficacy of the majority of NNRTIs-based treatments (Casado et al., 2000; Cozzi Lepri et al., 2000; Miller et al., 1998; Paredes and Clotet, 2010; Zhan et al., 2009). Therefore, improving the NNRTIs therapeutic spectra and differentiating the resistant mutation profiles may be the crucial key for the development of novel effective HAART regimens (Adamson and Freed, 2010; de Béthune, 2010; Paredes and Clotet, 2010; Shulman and Winters, 2003).

NNRTI interaction with the HIV-1 RT is a highly dynamic process (Zhan et al., 2009). Crystal structures of RT/NNRTI complexes showed that the drug interacts with a hydrophobic pocket (non-nucleoside inhibitors binding pocket or NNRTI-BP) (Schäfer et al., 1993; Ren and Stammers, 2008) formed mainly by the side chains of aromatic amino acids. Upon complexation, the NNRTI-BP changes its own conformation, leading to the inactivation of the enzyme itself. The NNRTI-BP adopts different conformations depending on the 3D features of the inhibitors and the amino acids side chain flexibility (Hsiou et al., 1996; Kohlstaedt et al., 1992). Moreover, mutations of some amino acids cause structural variations of the NNRTI-BP, which ultimately result in reduced affinities towards to most of the inhibitors (Esnouf et al., 1995; Patel et al., 1995; Ragno et al., 2005; Ren et al., 1995). In addition, HIV-1 RT itself also undergoes a conformational reorganization upon interaction with its substrates template-primer (TP) and deoxynucleoside triphos-

* Corresponding author. Tel.: +39 090 6766412; fax: +39 090 6766402.
** Corresponding author. Tel.: +39 0382 546354; fax: +39 0382 422286.
E-mail addresses: chimirri@pharma.unime.it (A. Chimirri), maga@igm.cnr.it (G. Maga).

0166-3542/$ – see front matter © 2010 Elsevier B.V. All rights reserved.
doi:10.1016/j.antiviral.2010.03.008

phate (dNTP), so that three structurally distinct mechanistic forms can be recognized in the reaction pathway catalyzed by HIV-1 RT: the free enzyme, the binary complex of RT with the template-primer (RT/TP), and the catalytically competent ternary complex of RT with both nucleic acid and dNTP (RT/TP/dNTP) (Huang et al., 1998; Jacobo-Molina et al., 1993). This means that the NNRTI-BP might not be identical in these three mechanistic forms. Several kinetic studies have shown that this is indeed the case, so that some NNRTIs selectively target one or a few of the different enzymatic forms along the reaction pathway (Maga et al., 2000). Indeed, it has been shown that a "communication" exists between the NNRTI-BP and the nucleotide binding site, so that some NRTI resistance mutations can influence NNRTI binding and vice versa (Blanca et al., 2003; Crespan et al., 2005; Paolucci et al., 2007). It was also observed that, while the majority of NNRTIs acted as non-competitive inhibitors, whose interactions with the RT allosteric pocket was not influenced by the vicinal incorporation of the enzyme substrates (Althaus et al., 1993a,b; de Béthune, 2010; Ren et al., 2000a,b), some NNRTIs showed different binding affinities to the enzyme in complex with its TP and/or dNTP substrates, behaving as mixed inhibitors (Fletcher et al., 1995; Maga et al., 2000; Samuele et al., 2009).

On the basis of a 3D pharmacophore model and the extensive structure–activity relationship (SAR) we have previously reported (Barreca et al., 2005, 2007; Monforte et al., 2008) the identification of new effective benzimidazol-2-ones NNRTIs. From the original scaffold, a series of new highly flexible molecules was derived showing major ability to elude the most clinically relevant RT drug resistance mutations (Monforte et al., 2009, 2010). Docking studies have shown that the novel benzimidazolone derivatives bind in a similar fashion to efavirenz (Monforte et al., 2010). However, the ability of the methyl groups of CHI-452 to occupy the hydrophobic space near the "roof" of the NNRTI-BP (consisting of P95, Y181, Y188, and W229), creates additional intermolecular interactions, thus explaining its high potency of inhibition. However, one mutation that still significantly reduced the potency of inhibition of these novel benzimidazolone derivatives was the K103N substitution. In order to improve these molecules through rational design, it would be important to understand in details their interaction with the mutated RT. Unfortunately, molecular docking was not helpful in elucidating the mechanism of interaction of these compounds with the K103N mutant, since it is well known that this mutation has a minimal influence on the bound conformation of NNRTIs, while it significantly affects the kinetics of the inhibitor-binding process, which is outside the investigational power of molecular docking.

Thus, in order to shed light on the mechanism of inhibition towards the K103N mutant, we sought to characterize and investigate in detail the kinetics of interaction of two N1 alkyl-phenyl sulfonyl -6-chloro- benzimidazol-2-ones, CHI-452 and CHI-465 (Fig. 1) with the three different mechanistic forms of the wild type and K103N mutant HIV-1 RT.

2. Materials and methods

2.1. Chemicals

All the reagents were of analytical grade and purchased from Sigma–Aldrich (St. Louis, MO), Merck Sharp & Dohme (Readington, NJ), ICN (Research Products Division, Costa Mesa, CA), or AppliChem GmbH (Darmstadt, Germany). Radioactive 2′deoxythymidine 5′-triphosphate [^{3}H]dTTP (40 Ci/mmol) was purchased from Amersham Bio-Sciences (GE Healthcare, Buckinghamshire, GB), while unlabeled dNTPs were from Boehringer Ingelheim GmbH (Ingelheim, Germany). GF/C filters were provided by Whatman Int. Ltd., (Maidstone, England).

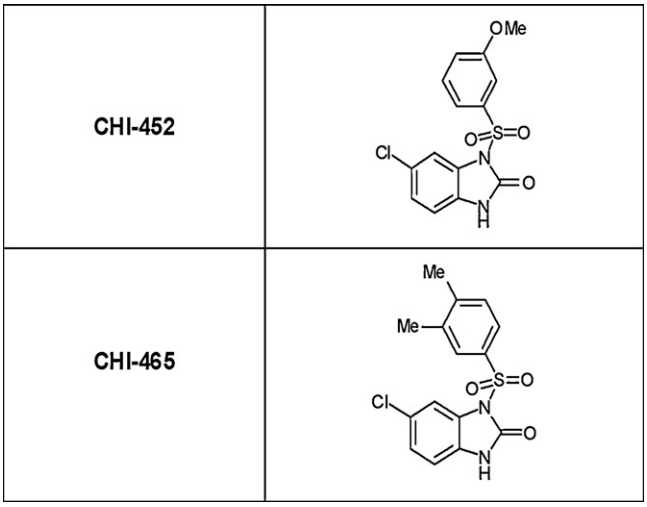

Fig. 1. Structures of the compounds used in this study.

2.2. Chemistry

Derivatives CHI-452 and CHI-465 were prepared as previously reported (Monforte et al., 2010).

2.3. Nucleic acid substrates

The homopolymer poly(rA) and the oligomer oligo(dT)$_{12–18}$ (Pharmacia & Upjohn Inc., Pfizer, Peapack, NJ) were mixed at weight ratios in nucleotides of 10:1 with 25 mM Tris–HCl (pH 8.0) containing 22 mM KCl, heated at 70 °C for 5 min and then slowly cooled at room temperature.

2.4. Expression, purification and cloning of recombinant HIV-1 RT forms

Recombinant heterodimeric RT, either wild type (wt) or the K103N variant were expressed and purified as briefly described below.

The HIV-1 RT gene fragment spanning codons 2–261 carrying the K103N mutation was amplified by PCR, digested with Acc1 and Pvu2 restriction enzymes and cloned into the expression plasmid p6HRT (ΔXho1/Bgl2). The resulting constructs were used for the production in *Escherichia coli* (BL21) and purification of recombinant His-tagged RT enzymes in a Fast Protein Liquid Chromatography (F-PLC) system, using Ni-NTA superflow column (QIAGEN, Valencia, CA) and Q-Sepharose column (Pharmacia, Sweden). All the enzymes were purified to a >95% purity, as confirmed by sodium dodecyl sulfate-polyacrylamide gel electrophoresis and Gelcode Blue stain, and had a specific activity for poly(rA)/oligo(dT) as template (primer). One Unit of DNA polymerase activity corresponds to the incorporation of 1 nmol of dNMP into acid-precipitable material in 60 min at 37 °C.

Western blotting confirmed the identity of the purified proteins by means of anti-RT or anti-His monoclonal antibodies.

2.5. HIV-1 RT RNA-dependent DNA polymerase activity assay

Poly(rA)/oligo(dT) was used as a template/primer for the RNA-dependent DNA polymerase reaction by HIV-1 RT, either wt or carrying the mutations. For the activity assay, a 25 μl final reaction volume contained TDB buffer (50 mM Tris–HCl (pH 8.0), 1 mM dithiothreitol (DTT), 0.2 mg/ml bovine serum albumine (BSA), 2% glycerol), 10 mM $MgCl_2$, 0.5 μg of poly(rA)/oligo(dT)$_{10/1}$ (0.3 μM 3′-OH ends), 10 μM ^{3}[H]dTTP 1 Ci/mmol and, finally, introduced

into tubes containing aliquots of different enzyme concentrations (5–10 nM RT). After incubation at 37 °C for indicated time, 20 μl from each reaction tube were spiked on glass fiber filters GF/C and, thereupon immediately, immersed in 5% ice-cold trichloroacetic acid (TCA) (AppliChem GmbH, Darmstadt). Filters were washed three times with 5% TCA and once with ethanol for 5 min, then dried and, finally, added with EcoLume® Scintillation cocktail (ICN, Research Products Division, Costa Mesa, CA), to detect the acid-precipitable radioactivity by PerkinElmer® Trilux MicroBeta 1450 Counter.

2.6. Steady-state kinetic assays

Steady-state kinetic assays were also performed to evaluate the activity of HIV-1 RT in the presence of fixed concentrations (IC_{50}), of selected inhibitors and variable concentrations of one of the two substrates (either poly(rA)/oligo(dT) or [^{3}H]TTP), while the other was maintained at saturating doses. [^{3}H]TTP concentrations varied between 0.2 and 20 μM, while poly(rA)/oligo(dT) doses ranged from 10 to 40 nM. These experiments led to the determination of V_{max}, K_m and k_{cat} parameters from Michaelis–Menten curves, as mentioned in the "calculation of kinetic parameters" section. The true inhibitor dissociation constant (K_i) values were derived as described.

2.7. Kinetic model

The mechanisms of action for the examined compounds were derived by the analysis of the effects observed on the different equilibria involved in the enzymatic reaction catalyzed by the HIV-1 RT.

A schematic drawing of these equilibria is depicted in Scheme 1. According to the ordered mechanism of the polymerization reaction, whereby the template-primer (TP) binds first, followed by the addition of dNTP, HIV-1 RT can be present in three different catalytic forms, as reported in the panel A: as a free enzyme (RT), in a binary complex with the TP (RT/TP), and in a ternary complex with TP and dNTP (RT/TP/dNTP). The resulting rate equation for such a system is very complex and impractical to use. For these reasons, the general steady-state kinetic analysis was simplified by varying one of the substrates (either TP or dNTP) while the other was kept constant. When the TP substrate was held constant at saturating concentration and the inhibition process at various concentrations of dNTPs was analyzed, at the steady-state all of the input RT was in the form of the RT/TP binary complex and only two forms of the enzyme (the RT/TP and the RT/TP/dNTP) could react with the inhibitor, as shown in the left part of the panel B. Similarly, when the dNTP concentration was kept constant at saturating levels and the inhibition at various TP concentrations was analyzed, RT was present either as a free enzyme or in the RT/TP/dNTP complex, as shown in the right part of the panel B.

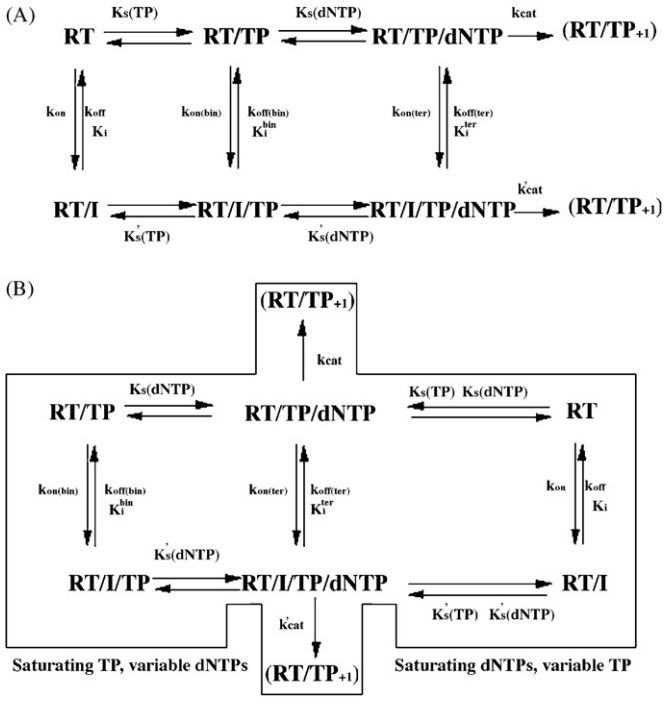

Scheme 1.

2.8. Kinetic parameter calculation

Values were calculated by non-least squares computer fitting of the experimental data to the appropriate rate equations.

Steady-state inhibitor binding was analyzed according to a non-competitive inhibition mechanism:

$$v = \frac{[V_{max}/(1 + I/K_i)]}{[1 + (K_m/S)]} \quad (1)$$

a mixed-type competitive inhibition:

$$v = \left\{ \frac{[V_{max}/(1 + I/K_i')]}{[1 + (K_m/S)]} \cdot \frac{[(1 + I/K_i)]}{[(1 + I/(K_i')]} \right\}. \quad (2)$$

or an uncompetitive mechanism:

$$v = \left\{ \frac{[V_{max}/(1 + I/K_i)]}{[1 + [K_m/(1 + I/K_i')]/S]} \right\} \quad (3)$$

The minimal reaction pathway for the HIV-1 RT reaction is illustrated in Scheme 1A. As shown in Scheme 1B, when TP was saturating (left part) $K_i = K_i^{free}$, whereas at saturating dNTP (right part), $K_i = K_i^{bin}$. In all cases, $K_i' = K_i^{ter}$. It follows that, if $K_i > K_i'$, then both K_m and V_{max} values will decrease at increasing inhibitor concentrations.

The true inhibition constant K_i was calculated under the conditions shown in Scheme 1B. For each inhibitor from the different enzymatic forms along the reaction pathway – free enzyme, binary complex with the TP and ternary complex with both the TP and the dNTP substrates – it was calculated from the variations of the $K_{i\,app}$ values as a function of varying concentrations of the TP or dNTP substrates, respectively, as follows:

$$K_{i\,app} = \left[1 + \left(\frac{K_m}{[S]}\right) K_i\right] \quad (4)$$

where [S] is the concentration of the variable substrate and K_m is the Michaelis constant.

The apparent binding rate values (k_{app}) were also evaluate from experimental data through the following exponential equation:

$$\frac{v_t}{v_0} = e^{-k_{app}\,t}$$

where t is the time.

$[E]_0$ being equal to the input enzyme concentration, $[E]_t$ to the enzyme able to react at the time point t, whereas $[E:I]_t$ the enzyme bound to the inhibitor at the time point t, it follows that:

$$[E]_t = [E]_0 - [E : I]_t$$

When $v_0 = k_{cat}[E]_0$ and $v_t = k_{cat}[E]_t$, it follows that $v_t/v_0 = 1 - [E : I]_t/[E]_0$. Therefore, the v_t/v_0 ratio is considered a linear function of $[E:I]_t$.

Table 1
Anti-enzymatic and antiviral activity of the compounds CHI-452 and CHI-465.

Compound	wt RT (IC_{50} μM)[a]	K103N RT (IC_{50} μM)	wt HIV-1		
			EC_{50} μM[a]	CC_{50} μM[a]	SI[a]
CHI-452	0.05 ± 0.01	10 ± 1	0.035 ± 0.014	>368.99	>10,543
CHI-465	0.004 ± 0.001	1.2 ± 0.1	0.006 ± 0.002	>371.14	>61,857
EFV	0.006 ± 0.001	0.8 ± 0.1	0.001 ± 0.0002	>6	>6000

[a] IC_{50}, concentration required to inhibit the enzymatic activity of HIV-1 RT by 50%; EC_{50}, concentration required to reduce by 50% the HIV-1-induced cytopathic effect; CC_{50}, concentration required to reduce by 50% the viability of uninfected cells; SI, selectivity index = CC_{50}/EC_{50}.

The k_{on} and k_{off} parameters, respectively indicating the association and the dissociation rates of the examined compounds towards the enzyme, were calculated according to the following equations:

$$k_{app} = k_{on}([I] + K_i) \quad (5)$$

$$k_{off} = k_{on}K_i \quad (6)$$

Since a competitive inhibitor binds to the enzyme only when this is complexed in the RT/TP form, it follows that $K_i^{free} = K_i^{bin}$, whereas the equilibrium dissociation constant from the ternary complex (K_i^{ter}), was calculated by the linear equation:

$$K_p = K_m\left[1 + \left(\frac{I}{K_i}\right)\right] \quad (7)$$

2.9. Data analysis and statistics

Data obtained were analyzed by linear or/and non-linear regression analysis using The GraphPad Software (San Diego, CA).

2.10. Antiviral and cytotoxicity assays.

The methodology of the anti-HIV assays was previously described (Monforte et al., 2010). Briefly, MT-4 cells infected with HIV-1 (IIIB) were transferred to microtiter plate wells, mixed with 100 μl of the appropriate dilutions of the test compounds, and further incubated at 37 °C. After five days the number of viable MT-4 cells was determined. The 50% effective concentration (EC_{50}) was defined as the concentration of compound required to reduce the virus-induced cytopathic effect by 50%. Similar experiments were carried out with mock-infected MT-4 cells to determine the concentration of the test compounds required to reduce the cell viability by 50% (CC_{50}). Cell viability was measured with standard MTS assays.

3. Results

3.1. Benzimidazol-2-one derivatives are potent inhibitors of HIV-1 RT

The compounds CHI-452 and CHI-465 (Fig. 1) showed excellent antiviral activity against the wild type HIV-1 virus in infected cells and very low toxicity, comparable or even better than the clinically approved efavirenz (Table 1). However, their potency was still reduced for the K103N RT mutant (Table 1). In order to understand the molecular basis for their interaction with the mutated RT, a detailed enzymological investigation was performed.

3.2. Benzimidazol-2-one derivatives show different mechanisms of inhibition towards HIV-1 RT wild type and the K103N mutant

In order to determine their exact mechanism of action, the RNA-dependent DNA polymerase activities of wt RT and the K103N mutant were measured in the presence of fixed concentrations of each inhibitor and variable concentrations of the nucleic acid or nucleotide substrate, respectively. Data were interpolated and the K_m, and V_{max} values were calculated according to Section 2.

In the case of the wt RT, the V_{max} values appeared to significantly decrease, whereas the K_m levels remained nearly identical for both the compounds and the substrates tested (data not shown), suggesting a fully non-competitive mechanism for both inhibitors (Eq. (1) in Section 2), so that their affinity for the non-nucleoside binding site (NNRTI-BP) was not influenced by the presence of the substrates.

For the mutant K103N, the K_m and the V_{max} values for the template/primer (TP) in the case of both inhibitors, and the K_m and the V_{max} values for the nucleotide (dNTP) substrate in the presence of compound CHI-452 were significantly decreased as the concentrations of the inhibitor increased (Table 2). This behavior is diagnostic of an uncompetitive mechanism of inhibition (described by Eq. (3) in Section 2), by which the inhibitor exhibited higher affinity towards the mutated enzyme when in complex with its substrates. Interestingly, when varying the dNTP substrate in the presence of compound CHI-465, the V_{max} values showed a dose-dependent reduction, whereas the K_m levels significantly increased (Table 2), indicating a mixed-type competitive inhibition (Eq. (2) of Section 2), whereby the affinity of the enzyme for the nucleotide substrate was partially reduced by the presence of the inhibitor. Thus, while both inhibitors were able to target all three enzymatic forms along the reaction pathway (free enzyme, binary complex with TP and ternary complex with TP and dNTP) with the same affinity in the case of the wild type enzyme, the presence of the K103N mutation rendered these three mechanistic forms non-equivalent in terms of inhibitor binding.

3.3. Benzimidazol-2-one derivatives show preferential binding to the K103N HIV-1 RT mutant in complex with its substrates

By applying the appropriate rate equations (see Section 2), the equilibrium dissociation constant (K_i) values for the two compounds from the different enzymatic forms along the reaction pathway were calculated (Table 3). In the case of wt RT, these values were derived from the variations of the V_{max} levels as a function of the inhibitor concentrations and were equal between the three catalytic forms of RT, according to the non-competitive mechanism of action shown by both compounds. The inhibitory potency of compound CHI-452 towards the K103N mutant, was increased by increasing concentrations of the TP and dNTP substrates. Thus, the equilibrium dissociation constants for the binary (K_i^{bin}) or ternary (K_i^{ter}) complexes of the enzyme for this inhibitor were obtained from the variations of the $K_{i\ app}$ values as a function of the TP and dNTP substrate concentrations, respectively (Fig. 2A and B), according to Eq. (4) (see Section 2 and Scheme 1). The equilibrium dissociation constant for the free enzyme (K_i^{free}) was then calculated from Eq. (3) (see Section 2). Compound CHI-465 showed a non-competitive mechanism only with respect to the nucleic acid, whereas it was partially competitive towards the dNTP. According to the kinetic pathway in Scheme 1, $K_i^{bin} < K_i^{free} < K_i^{ter}$. The true

Table 2
Variations of the K_m and V_{max} values of the K103N mutant for the nucleic acid (TP) and nucleotide (dNTP) substrates in the presence of the compounds CHI-452 and CHI-465.

Compound	Substrate			
	TP		dNTP	
	K_m (μM)	V_{max} (pmol min^{-1} nM^{-1})	K_m (μM)	V_{max} (pmol min^{-1} nM^{-1})
CHI-452 (μM)				
None	0.2 ± 0.1	1.3 ± 0.1	8 ± 0.8	1.2 ± 0.1
4	0.12 ± 0.02	0.7 ± 0.1	4.5 ± 0.5	0.6 ± 0.06
10	0.09 ± 0.02	0.5 ± 0.05	2 ± 0.3	0.4 ± 0.03
40	0.05 ± 0.01	0.2 ± 0.02	1.3 ± 0.1	0.2 ± 0.02
CHI-465 (μM)				
None	0.1 ± 0.01	1 ± 0.1	12 ± 1	0.9 ± 0.1
4	0.05 ± 0.01	0.55 ± 0.05	17 ± 2	0.6 ± 0.06
10	0.04 ± 0.006	0.4 ± 0.05	28 ± 3	0.45 ± 0.04
40	0.02 ± 0.005	0.2 ± 0.02	55 ± 5	0.3 ± 0.03

affinity of the inhibitor for the binary RT/TP complex (K_i^{bin}) was derived by the decrease of the $K_{i\ app}$ values as a function of the TP concentrations (Fig. 2C). The K_i^{ter} value was instead derived from the variation of the $K_{i\ app}$ a function of the dNTP substrate concentrations according to Eq. (4). The equilibrium dissociation constant for the free enzyme (K_i^{free}) was then calculated from Eq. (3) (see Section 2).

From the values reported in Table 3, it can be seen that both derivatives showed their highest affinity for either the ternary (CHI-452) or the binary (CHI-465) complexes of K103N with its substrates. The clinically approved NNRTI efavirenz was also included in this study for comparison (Table 3). While compound CHI-452 was less potent than efavirenz against the K103N mutant, compound CHI-465 showed affinities for the free enzyme and the ternary complex (K_i^{free} and K_i^{ter} values) similar to efavirenz, but displayed a 16-fold higher affinity towards the binary form of this mutant.

3.4. Effects of K103N resistance mutation on benzimidazol-2-one derivatives activity

In order to evaluate the resistance induced by the K103N mutation, the relative resistance index (RRI) was calculated, as the ratio $K_{i\ mut}/K_{i\ wt}$. The highest is the RRI value, the lowest the inhibitor affinity to the mutant with respect to the wild type enzyme. The three different catalytic forms of RT were examined. As shown in Fig. 3A, the mutation K103N reduced the affinities of all compounds tested, as indicated by RRI values >1. However, the data also clearly show that degree of resistance was different for the various enzymatic forms along the reaction pathway. In particular,

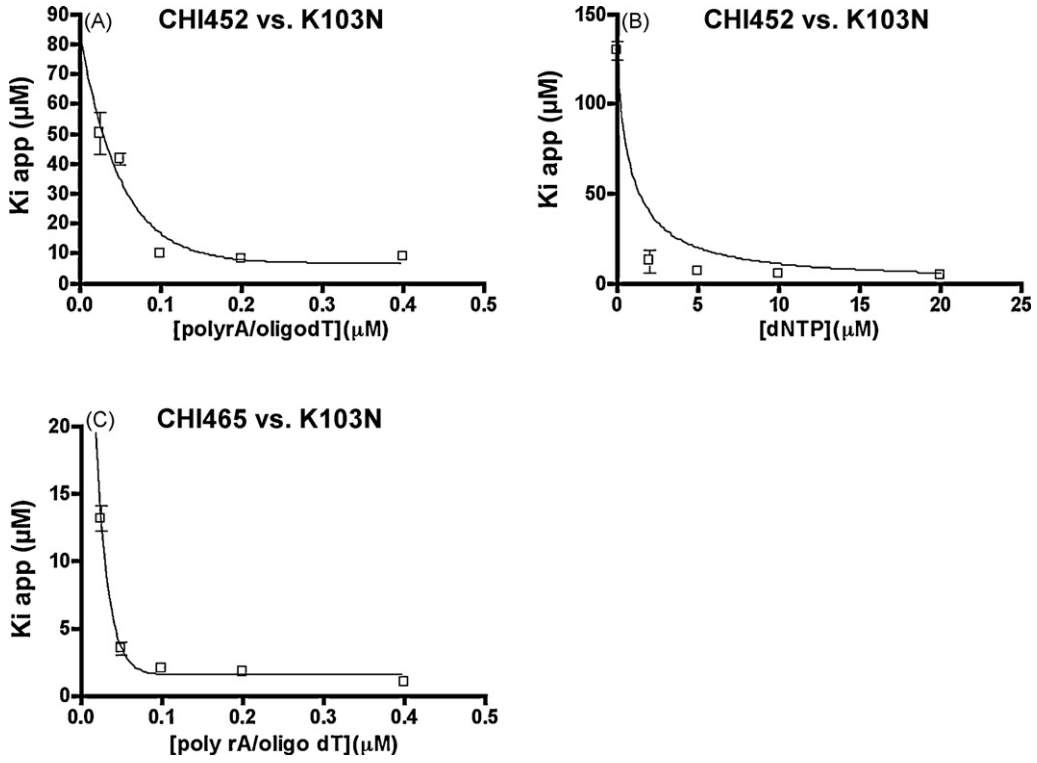

Fig. 2. The inhibitory potencies of CHI-452 and CHI-465 towards the K103N mutant are increased by the presence of the substrates. In all panels, data were from three independent replicates. Error bars indicate the mean values ± *S.D.* (A) Variation of the apparent equilibrium dissociation constant ($K_{i\ app}$) for CHI-452 binding to the K103N RT, as a function of increasing TP concentrations. Data were fitted to Eq. (4). (B) Variation of the apparent equilibrium dissociation constant ($K_{i\ app}$) for CHI-452 binding to the K103N RT, as a function of increasing dNTP concentrations. Data were fitted to Eq. (4). (C) Variation of the apparent equilibrium dissociation constant ($K_{i\ app}$) for CHI-465 binding to the K103N RT, as a function of increasing TP concentrations Data were fitted to Eq. (4).

Table 3
Kinetic parameters for the interaction of the CHI compounds with HIV-1 RT wild type and the drug resistant mutant K103N.

	[E]			[E:NA]			[E:DNA:dTTP]		
	K_i^{free} (μM)[a]	k_{on} (s^{-1} μM^{-1}) × 10^2	k_{off} (s^{-1}) × 10^2	K_i^{bin} (μM)[a]	k_{on} (s^{-1} μM^{-1}) × 10^2	k_{off} (s^{-1}) × 10^2	K_i^{ter} (μM)[a]	k_{on} (s^{-1} μM^{-1}) x10^2	k_{off} (s^{-1}) × 10^2
wt RT									
CH-452	0.052 (±0.005)	4.610 (±0.500)	0.240 (±0.025)	0.052 (±0.005)	9.870 (±0.990)	0.513 (±0.050)	0.052 (±0.005)	17.760 (±1.780)	0.924 (±0.092)
CHI-465	0.004 (±0.001)	37.190 (±3.720)	0.149 (±0.015)	0.004 (±0.001)	8.780 (±0.878)	0.035 (±0.004)	0.004 (±0.001)	10.800 (±1.080)	0.043 (±0.005)
EFV[b]	0.030 (±0.008)	1.000 (±0.100)	0.030 (±0.010)	0.030 (±0.007)	1.000 (±0.100)	0.030 (±0.003)	0.004 (±0.001)	4.000 (±0.200)	0.016 (±0.002)
K103N									
CHI-452	50.000 (±0.500)	0.010 (±0.001)	0.500 (±0.050)	8.000 (±0.800)	0.060 (±0.006)	0.480 (±0.050)	13.000 (±1.300)	0.013 (±0.0014)	0.180 (±0.020)
CHI-465	1.40 (±0.30)	0.0180 (±0.004)	0.025 (±0.005)	0.10 (±0.015)	0.030 (±0.002)	0.003 (±0.001)	1.400 (±0.015)	2.550 (±0.300)	3.570 (±0.360)
EFV[b]	1.500 (±0.200)	0.200 (±0.003)	0.300 (±0.030)	1.600 (±0.300)	0.250 (±0.050)	0.400 (±0.050)	0.800 (±0.010)	0.200 (±0.010)	0.160 (±0.01)

[a] K_i^{free}: dissociation equilibrium constant for the free enzyme [E]; K_i^{bin}: dissociation equilibrium constant for the binary complex between the enzyme [E] and the nucleic acid (either RNA or DNA) [NA]; K_i^{ter}: dissociation equilibrium constant for the ternary complex between the enzyme and NA/dNTP [E:NA:dTTP].
[b] EFV, efavirenz.

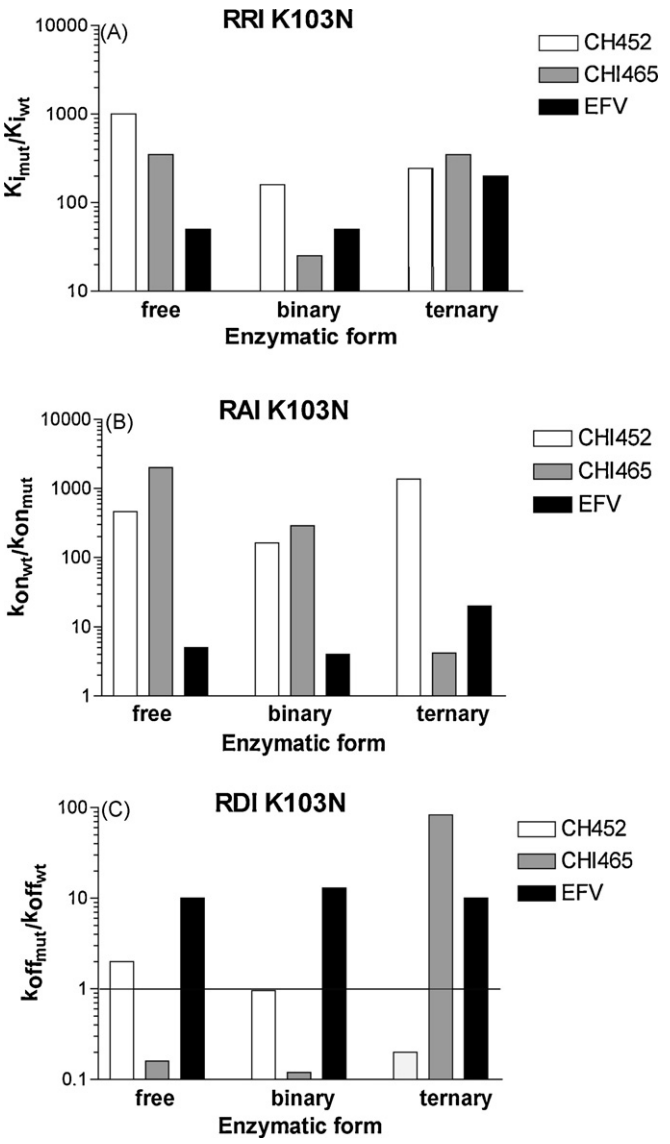

Fig. 3. The presence of the K103N mutation stabilizes the binding of CHI-465 to the RT-nucleic acid complex. (A) Relative resistance indexes (RRI), expressed as $K_{i\ mut}/K_{i\ wt}$, for the compounds CHI-452 (white bars), CHI-465 (gray bars) and efavirenz (EFV, black bars). The RRI values are expressed in a $\log_{10}$ scale. (B) Relative association indexes (RAI), expressed as $k_{on\ wt}/k_{on\ mut}$, for the compounds CHI-452 (white bars), CHI-465 (gray bars) and efavirenz (EFV, black bars). The RAI values are expressed in a $\log_{10}$ scale. (C) Relative dissociation indexes (RDI), expressed as $k_{off\ mut}/k_{off\ wt}$, for the compounds CHI-452 (white bars), CHI-465 (gray bars) and efavirenz (EFV, black bars). A reference line was drawn intersecting the *y*-axis at the value 1, corresponding to $k_{off\ mut} = k_{off\ wt}$.

compound CHI-465 showed a 2-fold lower RRI than efavirenz for the interaction with the binary complex of the mutated enzyme.

3.5. The K103N resistance mutation induces slow binding–tight binding interaction with the benzimidazol-2-one derivative CHI-465 to the viral RT

In order to shed light on the molecular mechanisms underlying the differential affinities of these inhibitors for the different enzymatic forms of the K103N mutant, we evaluated the corresponding association (k_{on}) and dissociation (k_{off}) rates for the free enzyme, the binary complex with the nucleic acid and the ternary complex with both the substrates, for wt RT and the K103N mutant (Table 3). Since the equilibrium dissociation constant K_i is related to these kinetic parameters by the relationship $K_i = k_{off}/k_{on}$, a reduced

affinity observed for the inhibitor to the enzyme (corresponding to an increase of the K_i value) may be associated with a decrease in the k_{on} values (slower association) or to an increase in the k_{off} values (faster dissociation). From the ratio between these two velocities for both the wt RT and the mutated enzyme, the relative association (RAI = $k_{on\ wt}/k_{on\ mut}$) or dissociation (RDI = $k_{off\ mut}/k_{off\ wt}$) indexes were thus calculated. With RAI or RDI values > 1, the inhibitor either binds to the mutated enzyme or dissociates from it more rapidly than in the case of wt RT. Conversely, RAI or RDI values <1, indicate a major selectivity of the inhibitor for the mutant enzyme with respect to the wild type. As shown in Fig. 3 B, the K103N mutation significantly decreased the association rates of all the CHI compounds to the enzyme, being all the RAI values >1. When the dissociation rates from the mutated enzyme were determined and compared to the corresponding values for wt RT (Fig. 3C), compound CHI-452 showed modestly reduced dissociation rates (1–2-fold) for the free enzyme and binary complex forms. Remarkably, this compound showed RDI values significantly <1 for the ternary complex, indicating that the K103N mutation rendered the binding by the inhibitor unexpectedly more stable to mutated enzyme, when complexed with its substrates, than to wt RT. This was also in agreement with the observed uncompetitive mechanism of action (Table 2). The compound CHI-465, on the other hand, showed RDI values <1 for the free enzyme and binary complex only, whereas its dissociation from the ternary complex of the mutated enzyme was significantly faster than from the corresponding complex with wt RT (RDI > 1). This was in agreement with the partially competitive mechanism of action observed with respect to the dNTP substrate (Table 2). The clinically approved efavirenz, on the other hand, showed RDI values > 10 for all the enzymatic forms, indicating a much faster dissociation of this compound from the K103N mutant with respect to the wt RT. Collectively, these data indicate that the K103N mutation causes resistance to the benzimidazol-2-one derivatives by reducing their association rates (slow binding), while these compounds were able to partially compensate this reduced binding by making very stable interactions with the mutated NNRTI-BP (tight binding), even stronger that with the wild type enzyme. This dual slow binding–tight binding mechanism of interaction was specific for these inhibitors, since efavirenz showed both slower association and faster dissociation rates from the K103N mutant, with respect to the wt RT.

4. Discussion

The benzimidazol-2-one class of NNRTIs has proven to be very effective in suppressing viral proliferation of wild type and mutated HIV-1 strains, comparably or even better than efavirenz (Monforte et al., 2009, 2010). However, these compounds still experienced a loss of potency similar to efavirenz against viruses with the K103N mutations. The K103N substitution is generally referred to as a "gatekeeper" mutation, able to increase the thermodynamic barrier for the "opening" of the NNRTI-BP by the incoming NNRTI, through the formation of an additional hydrogen bond (Ren et al., 2000a). Docking studies suggested that the interaction of benzimidazol-2-one derivatives with the wild type NNRTI-BP was similar, but not identical, to the one of efavirenz, but failed in elucidating the mechanism of resistance induced by the K103N mutation (Monforte et al., 2010). Thus, in order to rationalize the structure–activity relationships for these compounds, with the aim of making derivatives endowed with improved activity, it was of interest to understand the molecular basis for the resistance induced by the K103N mutation. In the present study, we sought to characterize and investigate in detail the mechanisms of interaction of two N1-substituted benzimidazol-2-one analogues (CHI-452 and CHI-465) in comparison with efavirenz, with the three different mechanistic forms of the viral wild type and the K103N mutant RT.

The most interesting result of this study was the observation that the mutation K103N greatly stabilized the binding of compound CHI-452 to the ternary complex and only slightly reduced the stability of the interaction of this compound with the other enzymatic forms (Fig. 3C). Compound CHI-465 showed a more stable binding to the free K103N enzyme and to the binary complex of the mutated RT with its nucleic acid substrate, but its binding was destabilized by the formation of the ternary complex. Efavirenz, on the other hand, showed faster dissociation rates from all the enzymatic forms of the K103N mutant with respect to the wild type enzyme. The K103N mutation causes a structural rearrangement of the NNRTI-BP, with a downward rotation of the W229 sidechain and the establishment of an hydrogen bond between the side chain of Y188 and the mutated K103N. Analysis of the structure of the K103N mutant in complex with efavirenz indicated that its binding within the mutated NNRTI-BP, perturbed the side chain movements of the W229 residue (Ren et al., 2000a). This structural element is part of the β12–β13 loop known as "primer grip" and involved in correct positioning of the primer for catalysis. Molecular docking of benzimidazol-2-one derivatives showed that they interact with the NNRTI-BP "roof" lined by residues P195, Y181, Y188 and W229 (Monforte et al., 2010). These interactions are maximized by the presence of dimethyl substituents, as in the case of CHI-465. Thus, it is possible that nucleic acid binding to the K103N mutant causes a spatial rearrangement of the NNRTI-BP residues which is optimal for interaction with the benzimidazol-2-one inhibitors. This would explain why these derivatives showed tighter binding to the K103N NNRTI-BP with respect to the wild type enzyme. As a result of the combination of the movement of the W229 residue, induced by the K103N mutation, and the strong interaction of CHI-465 with the W229 side chain, the primer grip might be locked into a conformation, which impairs the correct orientation of the 3′-OH primer for the in-line attack by the α-phosphate of the incoming dNTP. This, in turn, results in a slower open-to-close transition of the enzyme active site and in faster dNTP dissociation, hence explaining the partially competitive behavior of CHI-465 with respect to the nucleotide substrate.

The precise knowledge of the identity of the rate-limiting step for the binding of benzimidazol-2-one inhibitors to the K103N RT, will help to devise chemical modifications of their pharmacophoric group, aimed to overcome such limitation. Available structural and biochemical data, strongly support that the mutated N103 residue slows the k_{on} rate for inhibitor binding through the formation of an hydrogen bond with the Y188 side chain. Several strategies can been foreseen in order to circumvent this block. For example, it would be possible to increase the hydrogen bonding attitude of the inhibitor either with the protein main chain, as in the case of capravirine (Ren et al., 2000b), or specifically with the 103N side chain, as in the case of TMC-125 (Rodriguez-Barrios et al., 2005). Another possibility would be to increase the inhibitor's flexibility, as in the case of HBY-097 (Hsiou et al., 1998).

5. Conclusion

The benzimidazol-2-one derivatives studied here show the ability to interact more stably with the different enzymatic forms of the K103N mutant, achieving nearly 10-fold slower dissociation rates than in the case of the wild type enzyme (tight binding). Their absolute potencies, however, are still limited by a reduction in their association rate to the mutant (slow binding). The results of this study help to rationalize the mechanism of resistance of the K103N mutant towards benzimidazol-2-one derivatives and provides further information for the design of more effective new generation NNRTIs inhibitors with promising drug resistant profile and minimal toxicity.

Acknowledgements

This work has been partially supported by "Franca Rame and Dario Fo" Nobel Foundation grant-in-aid to AS. EC is the recipient of a FIRC 2008-2010 Fellowship.

References

Adamson, C.S., Freed, E.O., 2010. Novel approaches to inhibiting HIV-1 replication. Antiviral Res. 85, 119–141.

Althaus, I.W., Chou, J.J., Gonzales, A.J., Deibel, M.R., Chou, K.C., Kezdy, F.J., Romero, D.L., Aristoff, P.A., Tarpley, W.G., Reusser, F., 1993a. Steady-state kinetic studies with the non-nucleoside HIV-1 reverse transcriptase inhibitor U-87201E. J. Biol. Chem. 268, 6119–6124.

Althaus, I.W., Chou, J.J., Gonzales, A.J., Deibel, M.R., Chou, K.C., Kezdy, F.J., Romero, D.L., Palmer, J.R., Thomas, R.C., Aristoff, P.A., Tarpley, W.G., Reusser, F., 1993b. Kinetic studies with the non-nucleoside HIV-1 reverse transcriptase inhibitor U-88204E. Biochemistry 32, 6548–6554.

Balzarini, J., De Clercq, E., 1996. Analysis of inhibition of retroviral reverse transcriptase. Methods Enzymol. 275, 472–502.

Balzarini, J., Pelemans, H., Riess, G., Roesner, M., Winkler, I., De Clercq, E., Kleim, J.P., 1998. Retention of marked sensitivity to (S)-4-isopropoxycarbonyl-6-methoxy-3-(methylthiomethyl)-3,4-di hydroquin oxaline-2(1H)-thione (HBY 097) by an azidothymidine (AZT)-resistant human immunodeficiency virus type 1 (HIV-1) strain subcultured in the combined presence of quinoxaline HBY 097 and 2′,3′-dideoxy-3′-thiacytidine (lamivudine). Biochem. Pharmacol. 55, 617–625.

Balzarini, J., Van Laethem, K., Hatse, S., Vermeire, K., De Clercq, E., Peumans, W., Van Damme, E., Vandamme, A.M., Bölmstedt, A., Schols, D., 2004. Profile of resistance of human immunodeficiency virus to mannose-specific plant lectins. J. Virol. 78, 10617–10627.

Barreca, M.L., Rao, A., De Luca, L., Zappalà, M., Monforte, A.M., Maga, G., Pannecouque, C., Balzarini, J., De Clercq, E., Chimirri, A., Monforte, P., 2005. Computational strategies in discovering novel non-nucleoside inhibitors of HIV-1 RT. J. Med. Chem. 48, 3433–3437.

Barreca, M.L., De Luca, L., Iraci, N., Rao, A., Ferro, S., Maga, G., Chimirri, A., 2007. Structure-based pharmacophore identification of new chemical scaffolds as non-nucleoside reverse transcriptase inhibitors. J. Chem. Inf. Model. 47, 557–562.

Beale, K.K., Robinson Jr., W.E., 2000. Combinations of reverse transcriptase, protease, and integrase inhibitors can be synergistic in vitro against drug-sensitive and RT inhibitor-resistant molecular clones of HIV-1. Antiviral Res. 46, 223–232.

Blanca, G., Baldanti, F., Paolucci, S., Skoblov, A.Y., Victorova, L., Hübscher, U., Gerna, G., Spadari, S., Maga, G., 2003. Nevirapine resistance mutation at codon 181 of the HIV-1 reverse transcriptase confers stavudine resistance by increasing nucleotide substrate discrimination and phosphorolytic activity. J. Biol. Chem. 278, 15469–15472.

Casado, J.L., Hertogs, K., Ruiz, L., Dronda, F., Van Cauwenberge, A., Arnó, A., Garcia-Arata, I., Bloor, S., Bonjoch, A., Blazquez, J., Clotet, B., Larder, B., 2000. Non-nucleoside reverse transcriptase inhibitor resistance among patients failing a nevirapine plus protease inhibitor-containing regimen. AIDS 14, F1–F7.

Cozzi Lepri, A., Sabin, C.A., Staszewski, S., Hertogs, K., Müller, A., Rabenau, H., Phillips, A.N., Miller, V., 2000. Resistance profiles in patients with viral rebound on potent antiretroviral therapy. J. Infect. Dis. 181, 1143–1147.

Crespan, E., Locatelli, G.A., Cancio, R., Hübscher, U., Spadari, S., Maga, G., 2005. Drug resistance mutations in the nucleotide binding pocket of human immunodeficiency virus type 1 reverse transcriptase differentially affect the phosphorolysis-dependent primer unblocking activity in the presence of stavudine and zidovudine and its inhibition by efavirenz. Antimicrob. Agents Chemother. 49, 342–349.

de Béthune, M.P., 2010. Non-nucleoside reverse transcriptase inhibitors (NNRTIs), their discovery, development, and use in the treatment of HIV-1 infection: a review of the last 20 years (1989–2009). Antiviral Res. 85, 75–90.

Esnouf, R., Ren, J., Ross, C., Jones, Y., Stammers, D., Stuart, D., 1995. Mechanism of inhibition of HIV-1 reverse transcriptase by non-nucleoside inhibitors. Nat. Struct. Biol. 2, 303–308.

Fletcher, R.S., Syed, K., Mithani, S., Dmitrienko, G.I., Parniak, M.A., 1995. Carboxanilide derivative non-nucleoside inhibitors of HIV-1 reverse transcriptase interact with different mechanistic forms of the enzyme. Biochemistry 34, 4346–4353.

Hsiou, Y., Ding, J., Das, K., Clark Jr., A.D., Hughes, S.H., Arnold, E., 1996. Structure of unliganded HIV-1 reverse transcriptase at 2.7 Å resolution: implications of conformational changes for polymerization and inhibition mechanisms. Structure 4, 853–860.

Hsiou, Y., Das, K., Ding, J., Clark, A.D., Kleim, J.-P., Rösner, M., Winkler, I., Riess, G., Hughes, S.H., Arnold, E., 1998. Structures of Tyr188Leu mutant and wild-type HIV-1 reverse transcriptase complexed with the non-nucleoside inhibitor HBY 097: inhibitor flexibility is a useful design feature for reducing drug resistance. J. Mol. Biol. 284, 313–323.

Huang, H., Chopra, R., Verdine, G.L., Harrison, S.C., 1998. Structure of a covalently trapped catalytic complex of HIV-1 reverse transcriptase: implications for drug resistance. Science 282, 1669–1675.

Jacobo-Molina, A., Ding, J., Nanni, R.G., Clark Jr., A.D., Lu, X., Tantillo, C., Williams, R.L., Kamer, G., Ferris, A.L., Clark, P., Hizi, A., Hughes, S.H., Arnold, E., 1993. Crystal structure of human immunodeficiency virus type 1 reverse transcriptase complexed with double-stranded DNA at 3.0 Å resolution shows bent DNA. Proc. Natl. Acad. Sci. U.S.A. 90, 6320–6324.

Kohlstaedt, L.A., Wang, J., Friedman, J.M., Rice, P.A., Steitz, T.A., 1992. Crystal structure at 3.5 Å resolution of HIV-1 reverse transcriptase complexed with an inhibitor. Science 256, 1783–1790.

Maga, G., Ubiali, D., Salvetti, R., Pregnolato, M., Spadari, S., 2000. Selective interaction of the human immunodeficiency virus type 1 reverse transcriptase nonnucleoside inhibitor efavirenz and its thio-substituted analog with different enzyme–substrate complexes. Antimicrob. Agents Chemother. 44, 1186–1194.

Maggiolo, F., 2009. Efavirenz: a decade of clinical experience in the treatment of HIV. J. Antimicrob. Chemother. 64, 910–928.

Miller, V., de Béthune, M.P., Kober, A., Sturmer, M., Hertogs, K., Pauwels, R., Stoffels, P., Staszewski, S., 1998. Patterns of resistance and cross-resistance to human immunodeficiency virus type 1 reverse transcriptase inhibitors in patients treated with the nonnucleoside reverse transcriptase inhibitor loviride. Antimicrob. Agents Chemother. 42, 3123–3129.

Monforte, A.M., Rao, A., Logoteta, P., Ferro, S., De Luca, L., Barreca, M.L., Iraci, N., Maga, G., De Clercq, E., Pannecouque, C., Chimirri, A., 2008. Novel N1-substituted 1,3-dihydro-2H-benzimidazol-2-ones as potent non-nucleoside reverse transcriptase inhibitors. Bioorg. Med. Chem. 16, 7429–7435.

Monforte, A.M., Logoteta, P., Ferro, S., De Luca, L., Iraci, N., Maga, G., De Clercq, E., Pannecouque, C., Chimirri, A., 2009. Design, synthesis, and structure–activity relationships of 1,3-dihydrobenzimidazol-2-one analogues as anti-HIV agents. Bioorg. Med. Chem. 17, 5962–5967.

Monforte, A.M., Logoteta, P., De Luca, L., Iraci, N., Ferro, S., Maga, G., De Clercq, E., Pannecouque, C., Chimirri, A., 2010. Novel 1,3-dihydro-benzimidazol-2-ones and their analogues as potent non-nucleoside HIV-1 reverse transcriptase inhibitors. Bioorg. Med. Chem. 18, 1702–1710.

Paolucci, S., Baldanti, F., Campanini, G., Cancio, R., Belfiore, A., Maga, G., Gerna, G., 2007. NNRTI-selected mutations at codon 190 of human immunodeficiency virus type 1 reverse transcriptase decrease susceptibility to stavudine and zidovudine. Antiviral Res. 76, 99–103.

Paredes, R., Clotet, B., 2010. Clinical management of HIV-1 resistance. Antiviral Res. 85, 245–265.

Patel, P.H., Jacobo-Molina, A., Ding, J., Tantillo, C., Clark Jr., A.D., Raag, R., Nanni, R.G., Hughes, S.H., Arnold, E., 1995. Insights into DNA polymerization mechanisms from structure and function analysis of HIV-1 reverse transcriptase. Biochemistry 34, 5351–5363.

Ragno, R., Artico, M., De Martino, G., La Regina, G., Coluccia, A., Di Pasquali, A., Silvestri, R., 2005. Docking and 3-D QSAR studies on indolyl aryl sulfones. Binding mode exploration at the HIV-1 reverse transcriptase non-nucleoside binding site and design of highly active N-(2-hydroxyethyl)carboxamide and N-(2-hydroxyethyl)carbohydrazide derivatives. J. Med. Chem. 48, 213–223.

Ren, J., Stammers, D.K., 2008. Structural basis for drug resistance mechanisms for non-nucleoside inhibitors of HIV reverse transcriptase. Virus Res. 134, 157–170.

Ren, J., Esnouf, R., Garman, E., Somers, D., Ross, C., Kirby, I., Keeling, J., Darby, G., Jones, Y., Stuart, D., Stammers, D., 1995. High resolution structures of HIV-1 RT from four RT-inhibitor complexes. Nat. Struct. Biol. 2, 293–302.

Ren, J., Milton, J., Weaver, K.L., Short, S.A., Stuart, D.I., Stammers, D.K., 2000a. Structural basis for the resilience of efavirenz (DMP-266) to drug resistance mutations in HIV-1 reverse transcriptase. Structure 8, 1089–1094.

Ren, J., Nichols, C., Bird, L.E., Fujiwara, T., Sugimoto, H., Stuart, D.I., Stammers, D.K., 2000b. Binding of the second generation non-nucleoside inhibitor S-1153 to HIV-1 reverse transcriptase involves extensive main chain hydrogen bonding. J. Biol. Chem. 275, 14316–14320.

Rodriguez-Barrios, F., Balzarini, J., Gago, F., 2005. The molecular basis of resilience to the effect of the Lys103Asn mutation in non-nucleoside HIV-1 reverse transcriptase inhibitors studied by targeted molecular dynamics simulations. J. Am. Chem. Soc. 127, 7570–7578.

Samuele, A., Kataropoulou, A., Viola, M., Zanoli, S., La Regina, G., Piscitelli, F., Silvestri, R., Maga, G., 2009. Non-nucleoside HIV-1 reverse transcriptase inhibitors dihalo-indolyl aryl sulfones achieve tight binding to drug-resistant mutants by targeting the enzyme–substrate complex. Antiviral Res. 81, 47–55.

Schäfer, W., Friebe, W.G., Leinert, H., Mertens, A., Poll, T., von der Saal, W., Zilch, H., Nuber, B., Ziegler, M.L., 1993. Non-nucleoside inhibitors of HIV-1 reverse transcriptase: molecular modeling and X-ray structure investigations. J. Med. Chem. 36, 726–732.

Shulman, N., Winters, M., 2003. A review of HIV-1 resistance to the nucleoside and nucleotide inhibitors. Curr. Drug Targets Infect. Disord. 3, 273–281.

Sluis-Cremer, N., Arion, D., Parniak, M.A., 2000. Molecular mechanisms of HIV-1 resistance to nucleoside reverse transcriptase inhibitors (NRTIs). Cell Mol. Life Sci. 57, 1408–1422.

Zhan, P., Liu, X., Li, Z., Pannecouque, C., De Clercq, E., 2009. Design strategies of novel NNRTIs to overcome drug resistance. Curr. Med. Chem. 16, 3903–3917.